

University of Toronto
Faculty of Applied Science and Engineering

ECE422H1 Radio and Microwave Wireless Systems

Lab 1: Antenna Measurements

Prepared by Aurora Nowicki & Deniz Uzun

PRA0101 - January 24, 2024

2.1 Input Impedance and Resonant Frequency Measurement

1. Measure the length of the antenna and determine the approximate operating frequency of the antenna.

The length of the half-wave dipole antenna was measured to be $L = 12.5$ cm.

Since $L = \frac{\lambda}{2}$:

$$\lambda = 2L = 25 \text{ cm}$$

$$f = \frac{c}{\lambda} = \frac{2.998 \cdot 10^8 \text{ m/s}}{0.25 \text{ m}} = 1.1992 \cdot 10^9 \text{ Hz} \approx 1.2 \text{ GHz}$$

where c is the speed of light, λ is the wavelength and f is the frequency of the wave.

4. Press [FORMAT] and select Log Mag. 5. Press [MARKER] and set the marker to where the reflection coefficient of the antenna is lowest. Determine the -10 dB bandwidth.

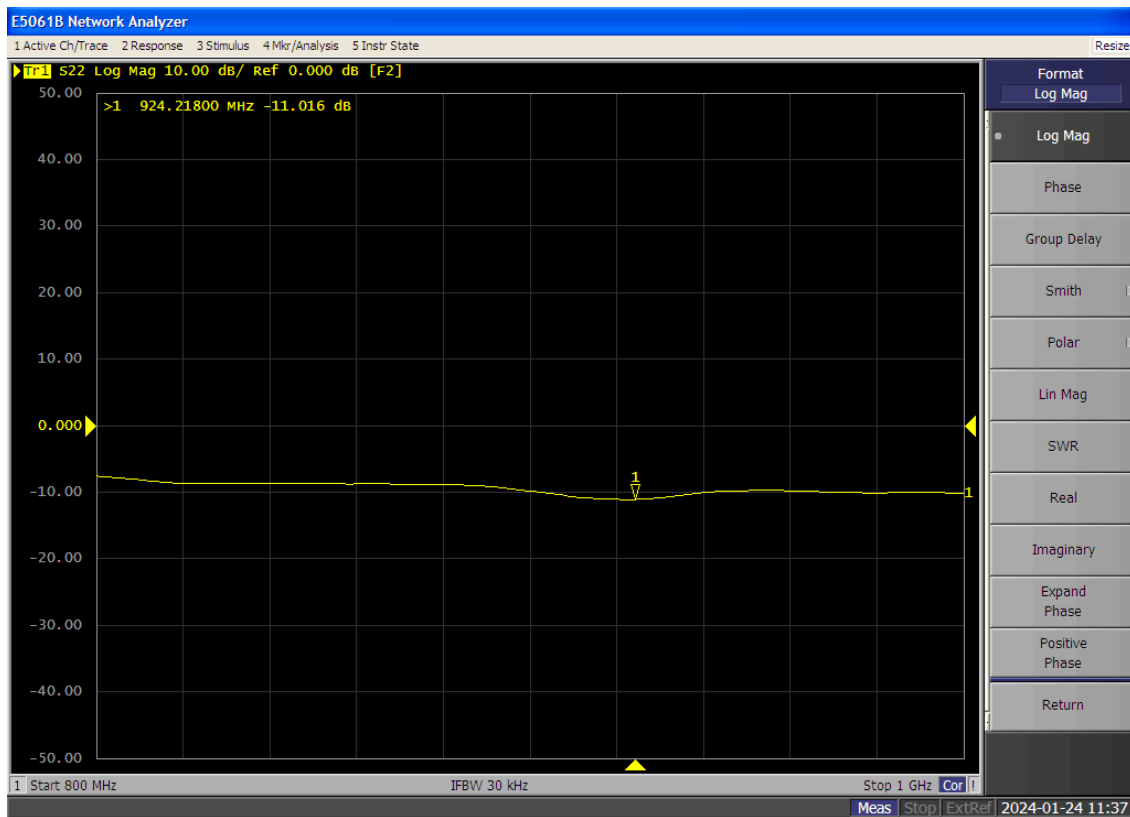


Figure 1: S22 Log Mag for the half-wave dipole antenna

By setting the marker where the reflection coefficient of the antenna is lowest, as shown in *Figure 1*, we determined the ideal frequency to be 924.218 MHz.

The frequencies, maximum and minimum, corresponding to the -10 dB BW from the graph in *Figure 1*, 940.298 MHz and 900.9 MHz were recorded, respectively. By taking the difference between these frequencies we determined the -10 dB bandwidth to be 39.398 MHz:

$$940.298 \text{ MHz} - 900.9 \text{ MHz} = 39.398 \text{ MHz}$$

We would expect the bandwidth of the half-wave dipole antenna to be much higher than this value. The error can be attributed to the signal from *Figure 1* not being strong enough at the time of measurement due to a poor connection.

6. Press [FORMAT] and select Smith to display the Smith Chart. Determine the frequency where the antenna is resonant; i.e., where the input reactance of the antenna is zero. Record the impedance and compare it to the expected value for a half-wave dipole.

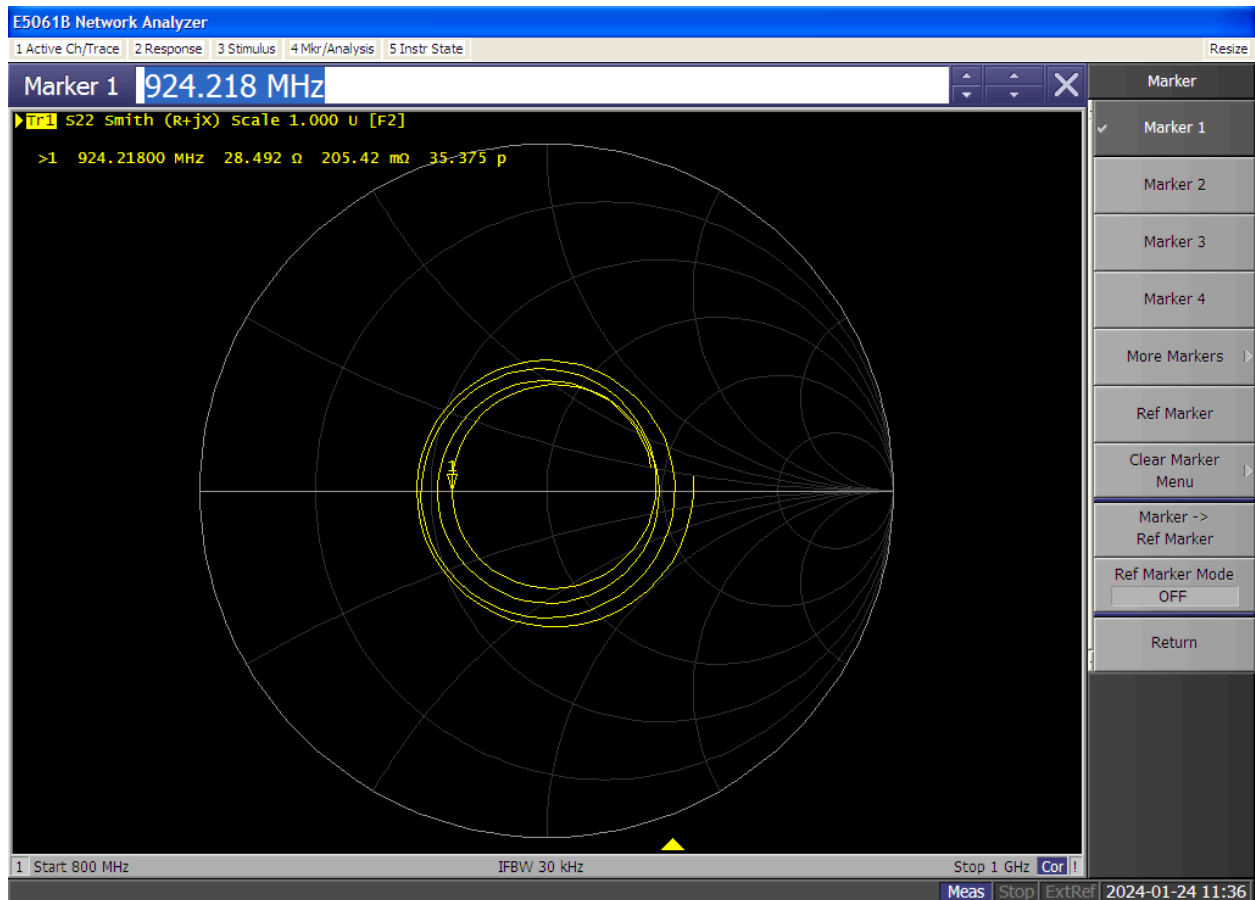


Figure 2: Smith Chart of the half-wave dipole antenna. The marker is set to 924.218 MHz frequency where the antenna is resonant.

From the Smith Chart in *Figure 2*, we determine the frequency where the antenna is resonant to be 924.218 MHz since at this point, the inductive and capacitive reactances of the antenna are equivalent (on X-axis of S.C.).

The input impedance at 924.218 MHz resonance was recorded to be 28.492 Ω .

The expected impedance for an ideal half-wave dipole antenna is $Z_{dipole} = 70 \Omega$ [1]

$$|Z_{ideal}| - |Z_{recorded}| = 41.508 \Omega$$

By comparing the magnitudes and phase angles of the recorded and ideal dipoles, we observe a significant difference. This deviation from the ideal input impedance can be attributed to the choice of resonant frequency, since the solution chosen was non-unique (there are many intersections of the plotted response with the real axis).

7. Measure the input reflection measurement of the Yagi antenna as well. Determine the -10 dB bandwidth. Does it have a wider or narrower bandwidth than the dipole?

By setting the marker where the reflection coefficient of the Yagi antenna is lowest in Log Mag mode, we determined the ideal frequency to be 941.906 MHz. The input impedance at 941.906 MHz was recorded to be 85.7 Ω .

The frequencies at maximum and minimum -10 dB were recorded to be 959.594 MHz and 819.296 MHz, respectively. By taking the difference between these frequencies we determined the -10 dB bandwidth to be 140.298 MHz. Since the bandwidth of the half-wave dipole was 39.398 MHz, Yagi antenna seems to have a wider bandwidth than the dipole. .

By moving the marker where the Yagi is resonant, as seen on *Figure 3*, we determined the frequency to be 941.906 MHz, which happens to be reasonably close to our dipole resonant frequency of 924.218 MHz.

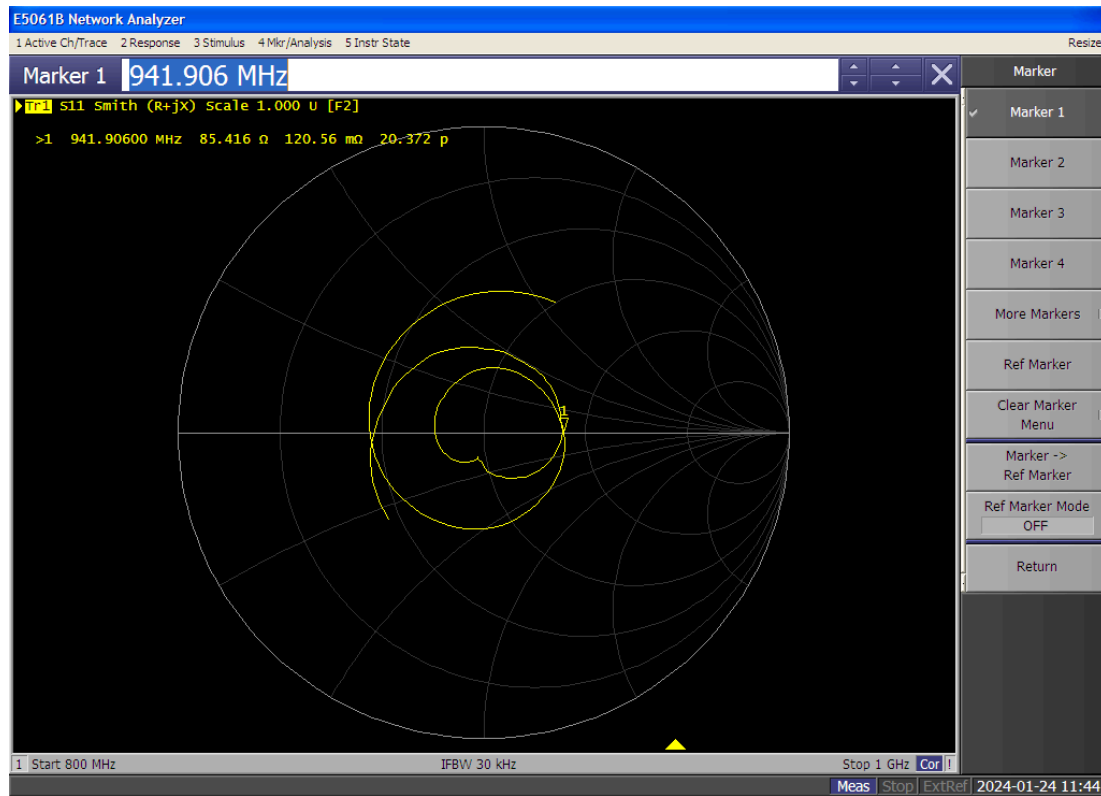


Figure 3: Smith Chart of the Yagi antenna. The marker is set to 941.906 MHz frequency where the Yagi antenna is resonant.

2.2 Pattern Measurement

2.2.1 E-Plane

Table 1: S_{21} (dB) measurements for E-plane co-polarization of the half-wave dipole antenna with respect to various angles of rotation in 15 degree increments

Angle (in degrees)	S_{21} (dB)	Normalized S_{21} (dB)
0	-39.4	-1.80
15	-38.8	-1.20
30	-44	-6.40
45	-40.9	-3.30
60	-42.3	-4.70
75	-43	-5.40
90	-44	-6.40
105	-48.1	-10.50
120	-44.6	-7.00
135	-43.7	-6.10
150	-44.5	-6.90
165	-45	-7.40
180	-41	-3.40
195	-40.7	-3.10
210	-40.2	-2.60
225	-43.4	-5.80
240	-45.5	-7.90
255	-50	-12.40
270	-55	-17.40
285	-50.4	-12.80
300	-45.1	-7.50
315	-42.5	-4.90
330	-43	-5.40
345	-41	-3.40

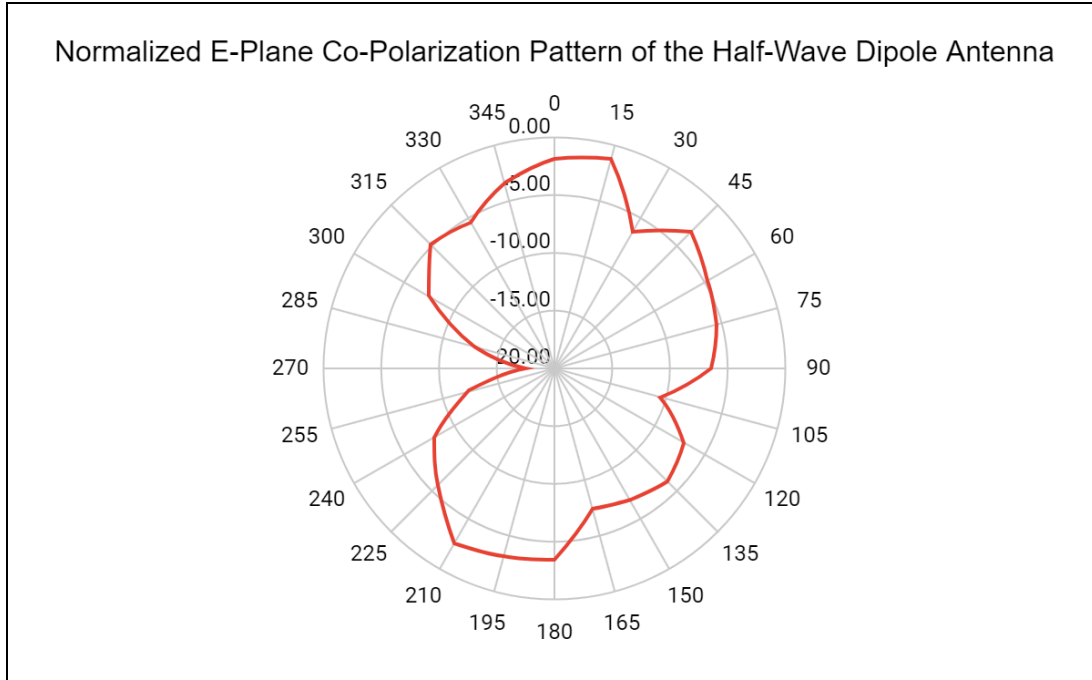


Figure 4: Normalized E-plane co-polarization pattern of the half-wave dipole antenna, plotted as a radar chart using the S_{21} (dB) measurements in Table 1.

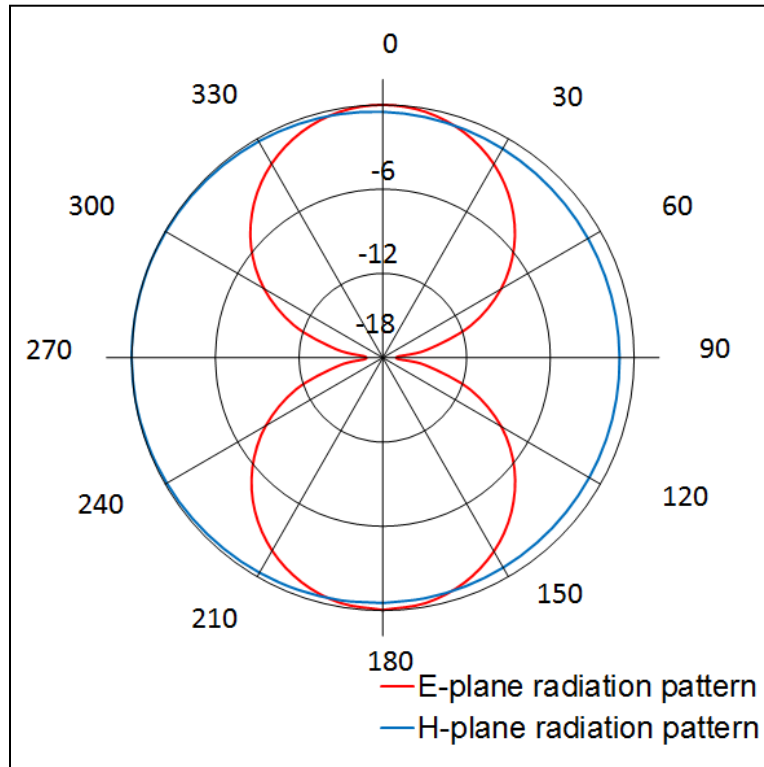


Figure 5: Theoretical E-plane and H-plane radiation patterns for half-wave dipole antenna [2]

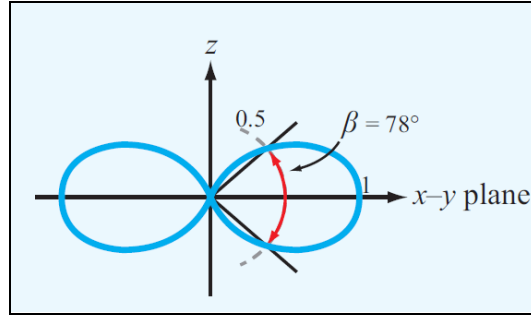


Figure 6: The radiation pattern of an ideal half-wave dipole [3]

Compare the measured E-plane pattern with the predicted pattern by plotting the theoretical pattern with a normalized version of your measurement. How do they compare?

Comparing Figures 4 and 5, the polarization pattern plotted from a normalized version of our measurement does not identically match with the theoretical one. These deviations are expected due to the imperfections and non-idealities of the experiment conditions. The general structure of the radiation pattern in Figure 4 resembles the theoretical E-plane pattern in Figure 5 since we can observe two circular patterns, dipping around 90 and 270 degrees.

2.2.2 H-plane

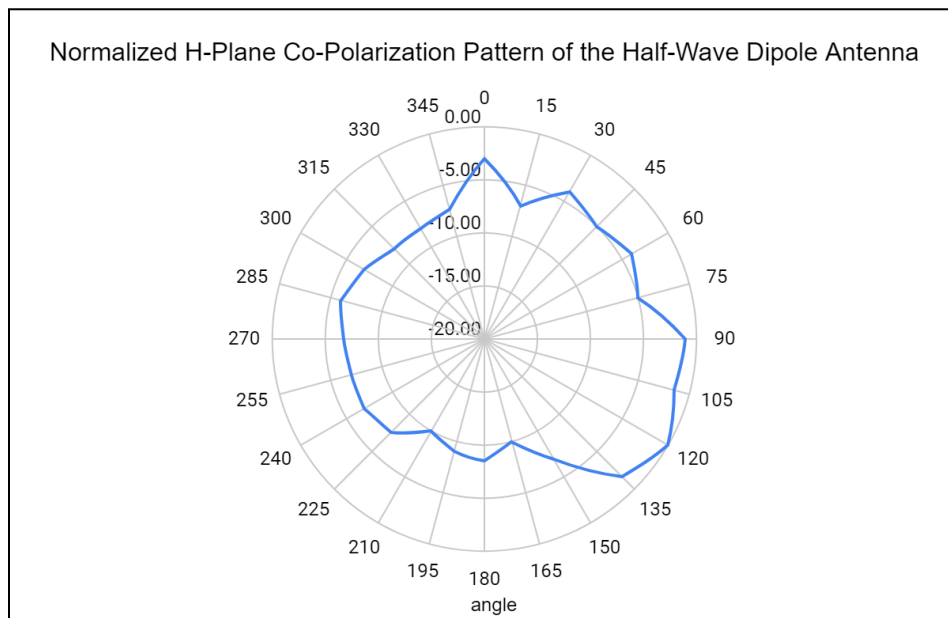


Figure 7: Normalized H-plane co-polarization pattern of the half-wave dipole antenna, plotted as a radar chart using the S_{21} (dB) measurements in Table 2.

Comment on the variation of the H-plane field pattern and compare that to what is expected.

Comparing Figures 7 and 5, the polarization pattern plotted from a normalized version of our measurement does not identically match with the theoretical one due to the imperfections and

non-idealities of the experiment conditions. The general structure of the radiation pattern in *Figure 7* resembles the theoretical H-plane pattern in *Figure 5* since we can observe a large circular pattern as expected.

Table 2: S_{21} (dB) measurements for H-plane co-polarization of the half-wave dipole antenna with respect to various angles of rotation in 15 degree increments

Angle (in degrees)	S_{21} (dB)	Normalized S_{21} (dB)
0	-38	-3.00
15	-42	-7.00
30	-39	-4.00
45	-40	-5.00
60	-39	-4.00
75	-40	-5.00
90	-36	-1.00
105	-36.5	-1.50
120	-35	0.00
135	-36.7	-1.70
150	-42	-7.00
165	-45	-10.00
180	-43.5	-8.50
195	-44	-9.00
210	-45	-10.00
225	-42.6	-7.60
240	-42	-7.00
255	-42	-7.00
270	-41.8	-6.80
285	-41	-6.00
300	-42	-7.00
315	-43	-8.00
330	-43	-8.00
345	-42.4	-7.40

2.2.3 Cross-polarization

Table 3: S_{21} (dB) measurements for E-plane co-polarization (co-pol) and cross-polarization (x-pol) of the half-wave dipole antenna with respect to various angles of rotation in 15 degree increments

Angle (in degrees)	S_{21} (dB) for Co-Pol	S_{21} (dB) for X-Pol	Difference in dB (X-Pol - Co-Pol)
0	-39.4	-46	-6.6
15	-38.8	-44	-5.2
30	-44	-47	-3
45	-40.9	-45	-4.1
60	-42.3	-44	-1.7
75	-43	-42.5	0.5
90	-44	-43	1
105	-48.1	-47	1.1
120	-44.6	-46	-1.4
135	-43.7	-56	-12.3
150	-44.5	-57	-12.5
165	-45	-57	-12
180	-41	-49	-8
195	-40.7	-47.5	-6.8
210	-40.2	-45.5	-5.3
225	-43.4	-42.7	0.7
240	-45.5	-42	3.5
255	-50	-41.6	8.4
270	-55	-42	13
285	-50.4	-47	3.4
300	-45.1	-51	-5.9
315	-42.5	-50	-7.5
330	-43	-50	-7
345	-41	-49	-8

Table 4: S_{21} (dB) measurements for H-plane co-polarization (co-pol) and cross-polarization (x-pol) of the half-wave dipole antenna with respect to various angles of rotation in 15 degree increments

Angle (in degrees)	S_{21} (dB) for Co-Pol	S_{21} (dB) for X-Pol	Difference in dB (X-Pol - Co-Pol)
0	-38	-43	-5
15	-42	-42.5	-0.5
30	-39	-40.7	-1.7
45	-40	-41.2	-1.2
60	-39	-39	0
75	-40	-37	3
90	-36	-39	-3
105	-36.5	-42	-5.5
120	-35	-39	-4
135	-36.7	-38.5	-1.8
150	-42	-36.2	5.8
165	-45	-35.5	9.5
180	-43.5	-36	7.5
195	-44	-36.2	7.8
210	-45	-38	7
225	-42.6	-38.6	4
240	-42	-39	3
255	-42	-40	2
270	-41.8	-42	-0.2
285	-41	-48	-7
300	-42	-47	-5
315	-43	-46	-3
330	-43	-48	-5
345	-42.4	-46.5	-4.1

Compare the values in this experiment with those from the co-polarization experiments. They should be at least an order of magnitude (10 dB) lower than those measured in the co-polarized experiment. Comment on what factors could have led to higher than expected cross-pol levels in your report.

Comparing the co-polarization (co-pol) and cross-polarization (x-pol) values in Table 3 for E-plane and Table 4 for H-plane, we can see that for most values the cross polarization gain is comparatively lower. However, the difference is not as much as -10dB except for a few highlighted values. We can attribute this to the antenna picking up interference from spurious radiation from other surrounding antennas. External factors such as reflections off of nearby objects or structures could also contribute to higher cross-polarization gain. Additionally mounting errors or misalignment of antenna elements may have led to increased coupling between co-polarized and cross-polarized measurements.

2.3 Additional Questions

- 1. Estimate the free space loss between the two antennas in your experiment, knowing the distance between the antennas (which you have recorded) and the gains of the antennas. The gain of the Yagi is approximately 7.3 dBi.***

The distance between the two tripods were measured to be $d = 75$ cm. We determined the ideal frequency to be $f = 924.218$ MHz for the half-wave dipole in Section 2.1. The gain of the half-wave dipole is approximately 2.15 dBi.

$$FSL = 20 \log(d) + 20 \log(f) + 20 \log\left(\frac{4\pi}{c}\right) - G_{\text{half-wave dipole}} - G_{\text{Yagi}}$$

$$FSL = 20 \log(0.75 \text{ m}) + 20 \log(924.218 \text{ MHz}) + 20 \log\left(\frac{4\pi}{2.998 \times 10^8 \text{ m/s}}\right) - 2.15 - 7.3$$

$$FSL = 57.934 \text{ dB}$$

- 2. What is the ratio between the co-pol to the x-pol at 0°?***

Ratio can be measured by subtracting dB values. The resulting power difference is 6.6 dB. Therefore we can conclude that the cross polarized antennas' power transfer is around 4 times lower than co-polarization radiation at 0 degrees.

$$\text{At } 0^\circ: E_{\text{co-pol}} = -39.4 \text{ dB and } E_{\text{x-pol}} = -46 \text{ dB}$$

$$E_{\text{co-pol}} - E_{\text{x-pol}} = -39.4 - (-46) = 6.6 \text{ dB}$$

3. *When measuring the input impedance, you will notice that it changes when an object is placed in close proximity to the antenna. Discuss how the impedance is affected by nearby objects and the underlying assumptions used in the impedance formula of the dipole. If you are an antenna designer for a cellphone company, discuss ways on how you would mitigate the problem of changing impedance. Also discuss any potential issues that may occur in the transceiver electronics when the impedance varies greatly.*

Nearby objects can introduce reflections which can cause standing waves and interference patterns that affect the impedance. They can also alter the effective electrical length of the antenna.

The underlying assumptions in the impedance formula for the dipole antenna include the assumption of free space, absence of nearby conductive objects and ideal conditions. As these assumptions are impossible to achieve in practical conditions, deviations from ideal in measurements are often expected.

As an antenna designer for a cellphone company you could mitigate this issue by designing an antenna tuner or adjustable matching network to the circuit at strategic points in the transmission line between the transceiver and the antenna to add or subtract the inductance or capacitance as seen at the receiving end as needed to counteract these environmental effects. Since the impedance of the antenna varies in response to objects, this change can be measured and opposed at the receiving end. Thus the effective impedance of the antenna can be engineered to remain matched to the source in varying conditions and limit the power loss due to reflections at the load.

When the impedance seen by the antenna varies greatly from the characteristic impedance of the RF power supply, mismatch losses can occur, which leads to reduced power transfer efficiency. Reduced power transfer efficiency can lead to increased ohmic losses, and result in potential overheating. Such large variations can also cause signal reflections back towards the transmitter, impacting the overall system performance.

3 Microstrip Patch Antenna

3.1 Input Impedance Measurement

7. Record the resonant frequency of the patch and the corresponding input impedance / input reflection coefficient.

The resonant frequency was recorded to be 930.65 MHz where the reflection coefficient of the antenna was at a minimum value of -10.7 dB (S_{11}). The corresponding input impedance was $90-j1.1 \Omega$.

8. You will now measure the impedance of the other input port. Swap the load and the cable and repeat 7. Verify that two ports have resonant frequencies that are close to each other.

The resonant frequency was recorded to be 934.35 MHz where the reflection coefficient of the antenna was at a minimum, verifying that the two ports have close resonant frequencies. The corresponding input impedance was recorded to be 88.3Ω .

3.2 E-plane Pattern Measurement

Table 5: S_{21} (dB) measurements for E-plane of the microstrip patch antenna with respect to various angles of rotation in 15 degree increments

Angle (in degrees)	S_{21} (dB)	Normalized S_{21} (dB)
0	-28	0
15	-28.3	-0.3
30	-28.8	-0.8
45	-29.3	-1.3
60	-31.7	-3.7
75	-36.5	-8.5
90	-39	-11
105	-40	-12
120	-38.1	-10.1
135	-37	-9
150	-36	-8
165	-37	-9
180	-44	-16
195	-45	-17
210	-44	-16
225	-46	-18
240	-48	-20
255	-44	-16
270	-47	-19
285	-43	-15
300	-42	-14
315	-39.7	-11.7
330	-33	-5
345	-30	-2

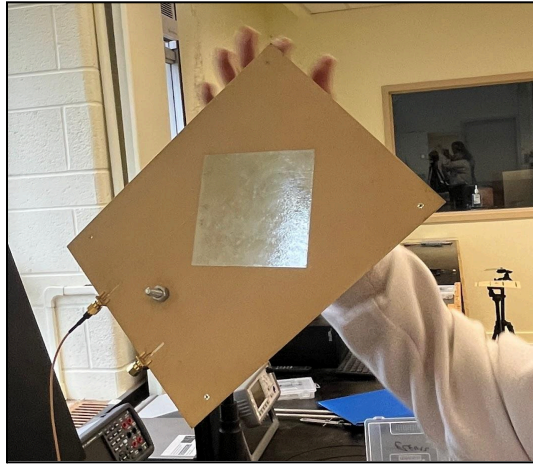


Figure 8: Microstrip patch antenna oriented along the E-plane

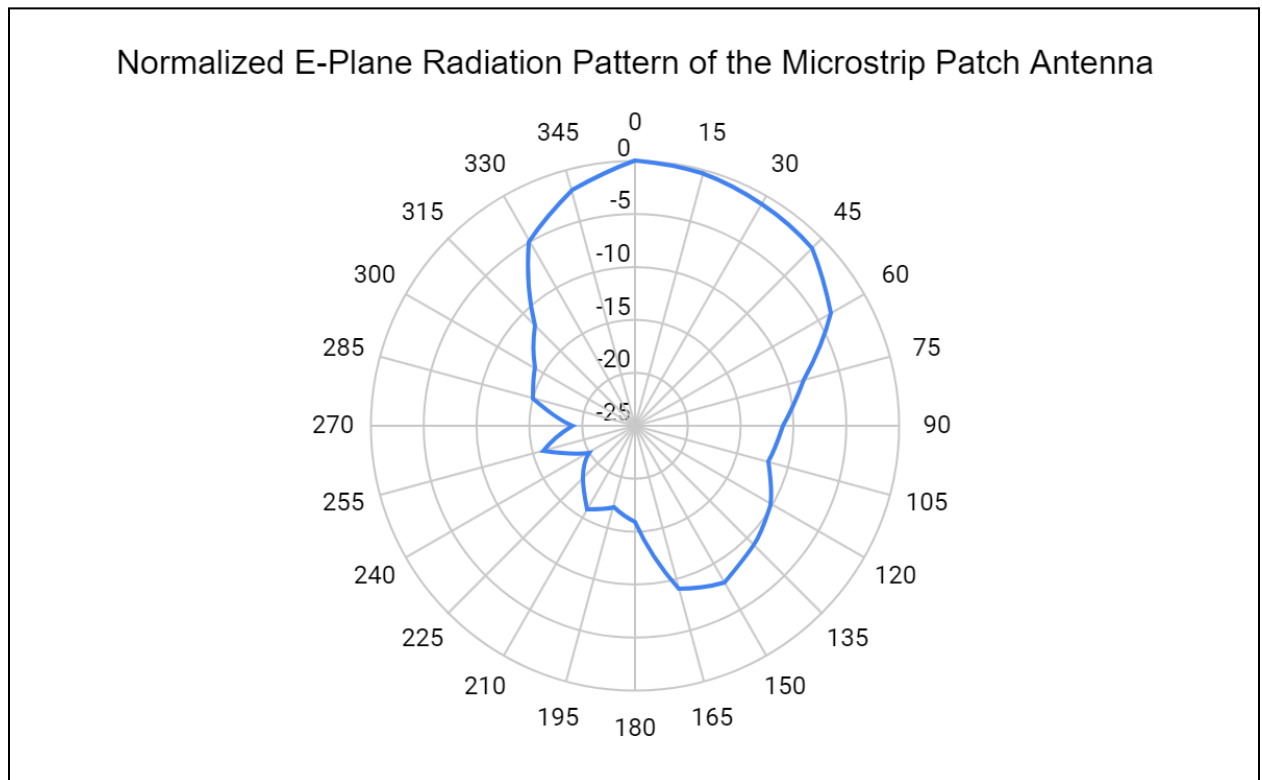


Figure 9: Normalized E-plane radiation pattern of the microstrip patch antenna, plotted as a radar chart using the S_{21} (dB) measurements in Table 5.

3.3 - H-plane Pattern Measurement

Table 6: S_{21} (dB) measurements for H-plane of the microstrip patch antenna with respect to various angles of rotation in 15 degree increments

Angle (in degrees)	S_{21} (dB)	Normalized S_{21} (dB)
0	-39	0
15	-40	-1
30	-43	-4
45	-42	-3
60	-39	0
75	-39	0
90	-40	-1
105	-46	-7
120	-60	-21
135	-63	-24
150	-56	-17
165	-52	-13
180	-47	-8
195	-46	-7
210	-45	-6
225	-48	-9
240	-51	-12
255	-44	-5
270	-60	-21
285	-44	-5
300	-39	0
315	-43	-4
330	-42	-3
345	-41	-2

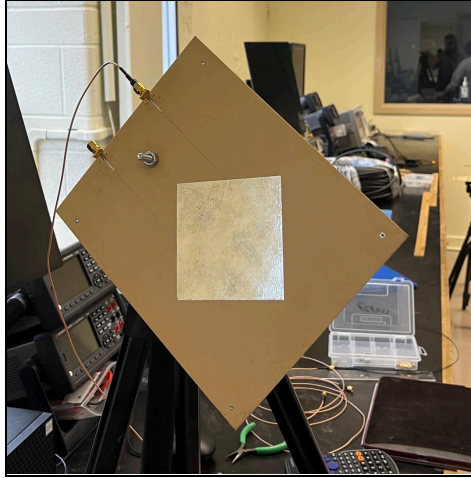


Figure 10: Microstrip patch antenna oriented along the H-plane

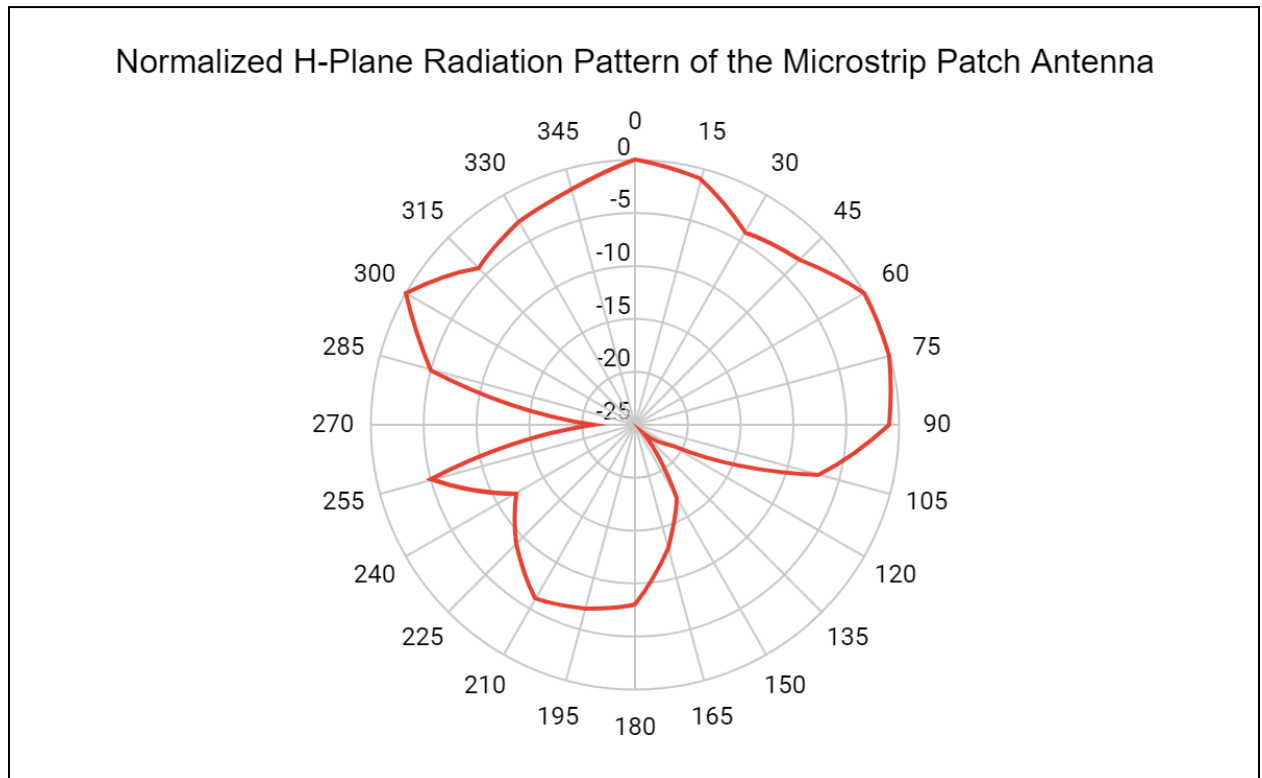


Figure 11: Normalized H-plane radiation pattern of the microstrip patch antenna, plotted as a radar chart using the S_{21} (dB) measurements in Table 6.

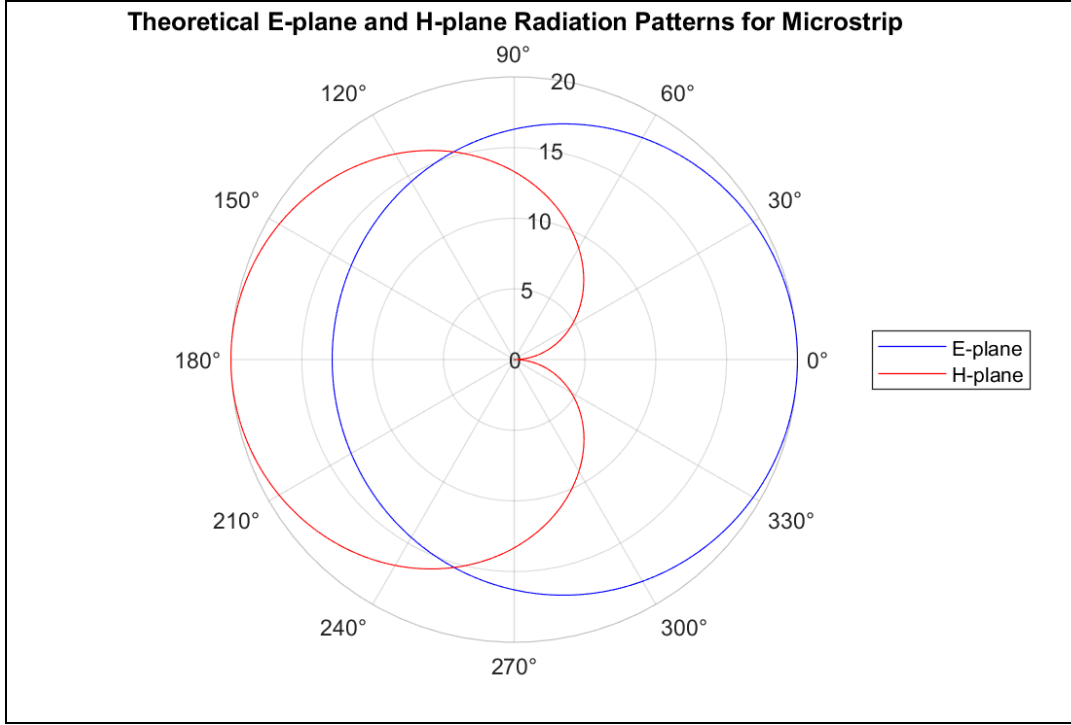


Figure 12: Theoretical E-plane and H-plane radiation patterns for microstrip patch antenna

1. **Comment on the radiation pattern of the antenna, based on your observations of the principal plane patterns of the patch. Compare the measured and theoretical radiation on the E- and H-planes.**

By comparing the radiation patterns in the E-plane in *Figures 9 and 12*, we can observe a circular pattern with smoother dips to the centre of the plot. The E-field pattern in the E-plane, $\theta = 90^\circ$, $0^\circ \leq \phi \leq 90^\circ$ and $270^\circ \leq \phi \leq 360^\circ$ is (up to a constant) is given by:

$$E_\phi = \frac{\sin\left(\frac{k_o h}{2} \cos \phi\right)}{\frac{k_o h}{2} \cos \phi} \cos\left(\frac{k_o L_e}{2} \sin \phi\right).$$

From *Figure 11*, for the radiation pattern in the H-plane, we observe minima at angles close to 135° and 270° . Ideally we would expect the minima to occur around 90° and 270° . By comparing it to the theoretical radiation pattern in *Figure 12*, we can observe the similar large and small lobes (front and back). The equation for the radiation pattern in the H-plane, $\phi = 0^\circ$, $0^\circ \leq \theta \leq 180^\circ$ is (up to a constant):

$$E_\phi = \sin \theta \frac{\sin\left(\frac{k_o h}{2} \sin \theta\right)}{\frac{k_o h}{2} \sin \theta} \frac{\sin\left(\frac{k_o W}{2} \cos \theta\right)}{\frac{k_o W}{2} \cos \theta},$$

Based on the MATLAB plot of this equation (see *Figure 12*) and comparing it to our measured data we can conclude that the measured radiation patterns of the antenna resembles the theoretical radiation patterns on the E- and H-planes in terms of antenna directivity characteristics.

2. **Using a free-space loss calculation, determine the approximate peak gain of the microstrip patch.**

$$FSPL = \left(\frac{4\pi df}{c}\right)^2 \frac{1}{G_{\text{microstrip patch}} * G_{\text{Yagi}}}$$

$$S_{21} = 20 \log(4\pi d) - 20 \log\left(\frac{c}{f}\right) - G_{\text{microstrip patch}} - G_{\text{Yagi}}$$

$$- 28 \text{ dB} = 20 \log(4\pi(0.75 \text{ m})) - 20 \log\left(\frac{2.998 * 10^8 \text{ m/s}}{930.65 \text{ MHz}}\right) - G_{\text{microstrip patch}} - 7.3 \text{ dB}$$

$$G_{\text{microstrip patch}} = 88.22 \text{ dB}$$

3.4 Linear Polarization

4. **Record the S_{21} value measured by the network analyzer.**

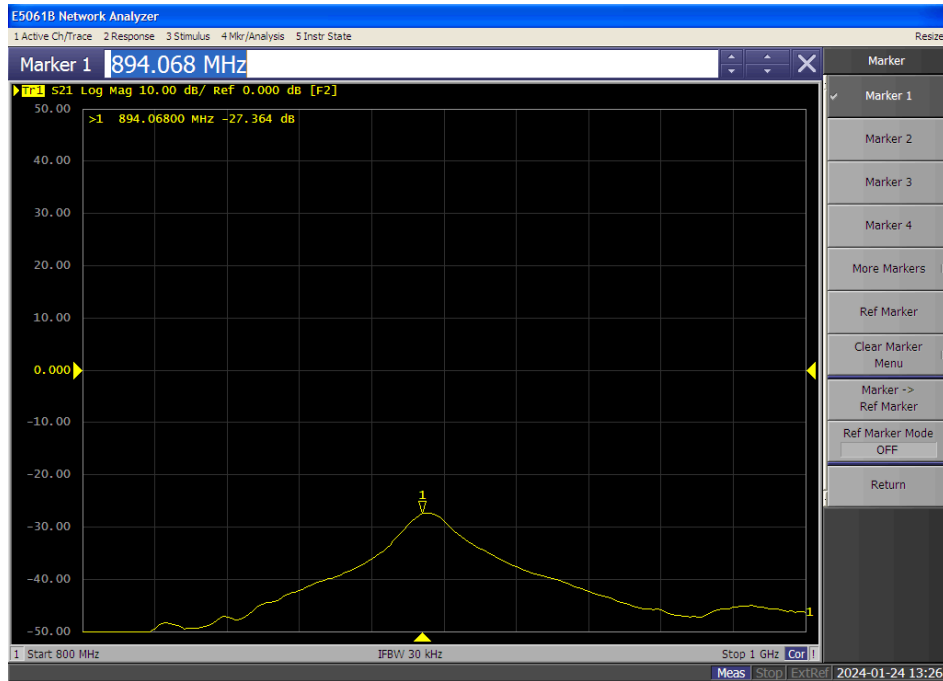


Figure 13: Center frequency of microstrip patch antenna with Wilkinson power divider configured to measure co-polarized E-field radiation pattern

From *Figure 13*, we have recorded: $S_{21} = - 27.364 \text{ dB}$

5. Rotate the patch by 90° , hence cross-polarizing the two antennas. 6. Record the S_{21} value measured by the network analyzer.

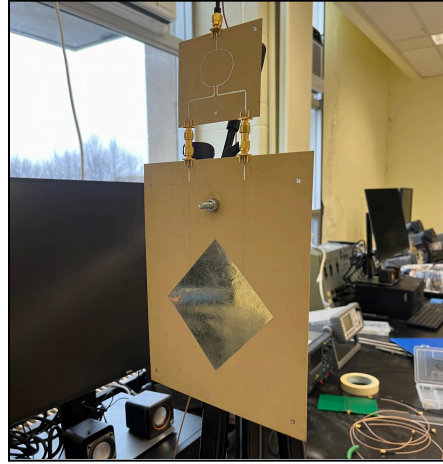


Figure 14: Microstrip patch antenna with a Wilkinson power divider; rotated 90° to cross-polarize the two antennas.

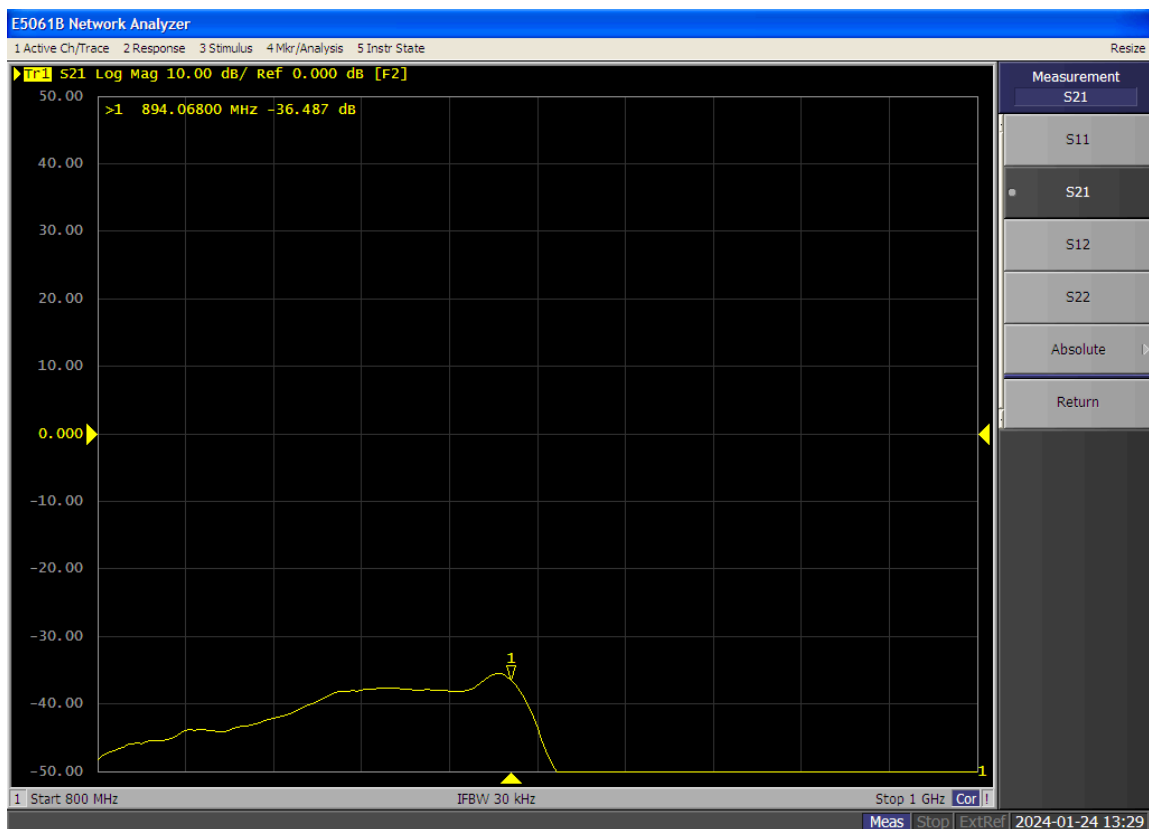


Figure 15: Center frequency of microstrip patch antenna with Wilkinson power divider configured to measure cross-polarized E-field radiation pattern

From Figure 15, we have recorded: $S_{21} = -36.487 \text{ dB}$

7. Compare the transmission levels (S_{21}).

By comparing our results, we observe that the gain of in-phase E-field propagation is greater when the two antennas are co-polarized. This is as expected, since microstrip antennas are symmetric and thus provide good performance in the co-polarized direction. When linearly polarized, the gain of the antenna is even greater but more directive, hence the large difference in co and cross-polarization power gain.

3.5 Circular Polarization

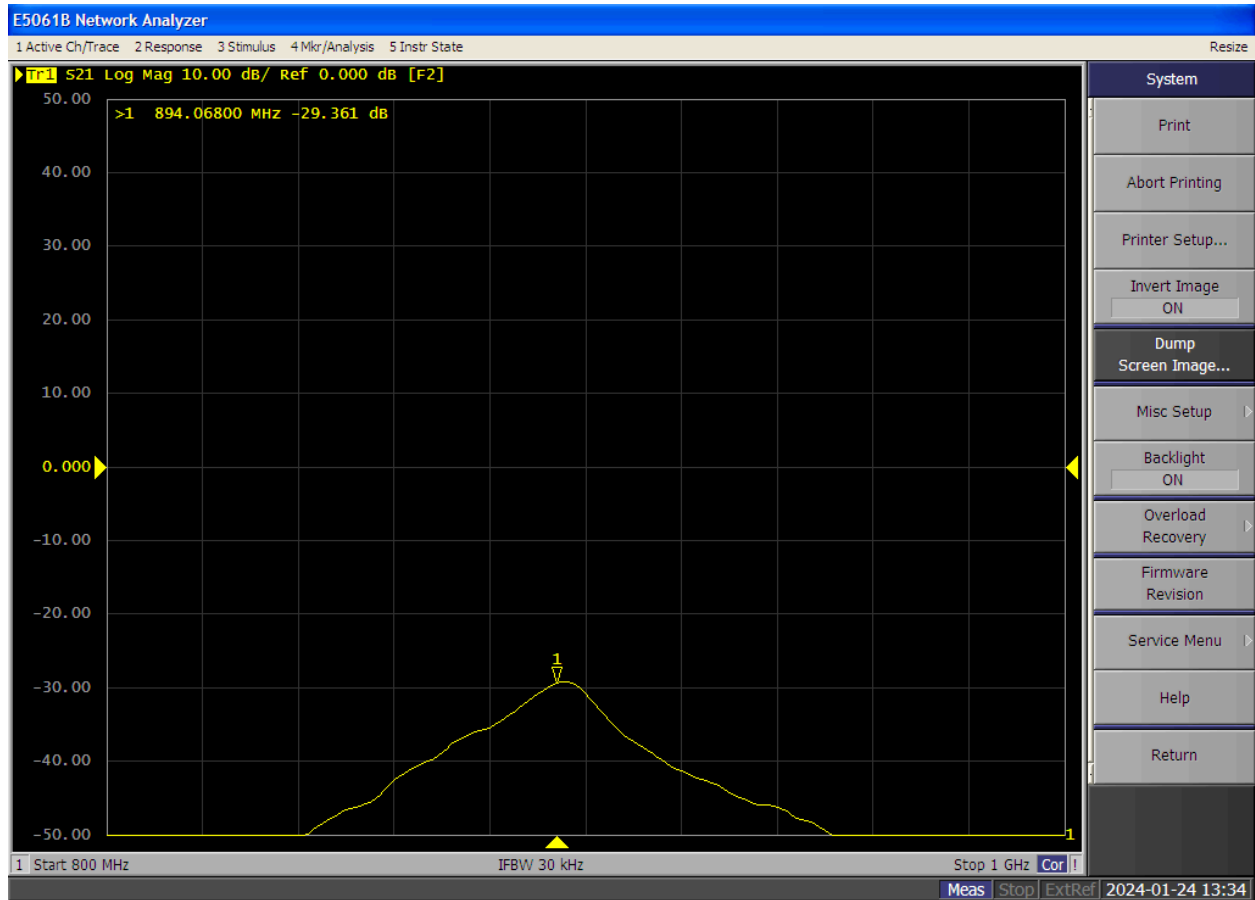


Figure 16: S_{21} measurement of microstrip patch antenna configuration with quadrature hybrid inserted. Similar values were obtained for both polarizations.

4. Record the S_{21} value measured by the network analyzer.

We have recorded: $S_{21} = -30.2 \text{ dB}$

5. Rotate the patch by 90° . 6. Record the S_{21} value measured by the network analyzer.

From Figure 16, we have recorded: $S_{21} = -29.361 \text{ dB}$

7. Compare the transmission levels (S_{21}). Do you expect a change when the patch is rotated? By how much? How does the measured power level compare to the linear-to-linear polarization case?

In circular polarization, the S_{21} values remained relatively constant despite the patch rotation, as expected. We do not expect much difference in gain between cross and co-polarized states in this case as opposed to the linear case, because the circular polarization of the microstrip receiving antenna caused by the 90 degree lag in input power to the patch means that the antenna should be less susceptible to the polarization of the directional antenna.

We notice, however, that the peak power gain in the circular polarization case is less than the power transferred in the co-polarized state when the antenna was linearly polarized. This was also expected, since the linear polarization creates a radiation pattern with more isotropic gain in one direction than the other.

References

- (1) S. V. Hum, "Half-wave Dipole" in Radio and Microwave Wireless Systems
- (2) "E-plane and H-plane radiation pattern of folded dipole antenna." ResearchGate.
[Online]. Available:
https://www.researchgate.net/figure/E-plane-and-H-plane-radiation-pattern-of-folded-dipole-antenna_fig4_286651403. [Accessed: January 31, 2024].
- (3) F. T. Ulaby and U. Ravaioli, "Fundamentals of Applied Electromagnetics," 8th ed. Prentice Hall, 2014, ch. 9, Fig. 9-17.